A Weak Interaction between Iron and Uranium in Uranium Alkyl Complexes Supported by Ferrocene Diamide Ligands

Marisa J. Monreal and Paula L. Diaconescu*

Department of Chemistry & Biochemistry, University of California, Los Angeles, California 90095

Received June 1, 2007

Alkyl complexes of uranium supported by ferrocene diamide ligands are described along with the corresponding cationic species. Synthesis of uranium dialkyl compounds fc(NSi^{t}BuMe$_2$)$_2$UR$_2$ [R = Np (*neo*-pentyl), Bz (benzyl)] was accomplished by salt metathesis between fc(NSi^{t}BuMe$_2$)$_2$UI$_2$(THF) and *neo*-pentyl lithium or benzyl potassium. Protonation of one alkyl ligand led to the isolation of a cationic uranium alkyl complex. DFT calculations and X-ray crystallography data support the existence of a donor–acceptor, weak interaction between iron and uranium.

The organometallic chemistry of uranium has been dominated by cyclopentadienyl complexes.[1,2] Recently, new reactivity patterns, beyond those of d elements, have been reported for noncyclopentadienyl complexes.[3–6] Similarly, although alkyl complexes of uranium(IV) have been investigated for cyclopentadienyl systems,[7–13] systems supported by other ancillary ligands are increasingly studied.[14–18] We are interested in exploiting ferrocene 1,1′-disubstituted ligands as versatile frameworks to support uranium(IV) alkyl moieties. Such ligands have the following characteristics: (i) the 1,1′-disubstituted ferrocene enforces cis-coordination of the two donors, thus only one side of the metal center is blocked; (ii) the ferrocene backbone has the ability to accommodate changes in the electronic density at a metal center by varying the geometry around iron;[19] and (iii) a weak interaction of donor–acceptor type[19–23] could occur between iron and uranium that might influence the reactivity of the complex. Incorporation of electron-rich ferrocene ligands has been shown[19] to stabilize a highly reactive, cationic titanium species, an example of a d^0 metal compound. To this end, we synthesized *mono*(1,1′-diamidoferrocene) complexes of tetravalent uranium and report our studies on the interaction between uranium and iron in a cationic benzyl complex.

Results and Discussion

The reaction between UI$_3$(THF)$_4$[24] and [K$_2$(OEt$_2$)$_2$]-fc(NSi^{t}BuMe$_2$)$_2$[25] in tetrahydrofuran led to a mixture of compounds, U(fc(NSi^{t}BuMe$_2$)$_2$)$_2$ and fc(NSi^{t}BuMe$_2$)$_2$UI$_2$-(THF) (**1-I$_2$(THF)**), from which the latter was separated as a consequence of its insolubility in hexanes. Both products obtained are uranium(IV) compounds, a common occurrence when starting from UI$_3$(THF)$_4$;[26,27] presumably, uranium(III) disproportionates to uranium(IV) and some form of uranium(0), which is removed by filtration. Several reports show that employing a stoichiometry consistent with this disproportionation reaction increases the yield of the uranium(IV) product.[26,27] Optimization of the reaction conditions allowed the isolation of **1-I$_2$(THF)** in 60% yield reproducibly. Reactions between compound **1-I$_2$(THF)** and alkyl sources (benzyl potassium, *neo*-pentyl lithium) led to uranium dialkyl complexes (Scheme 1, only the uranium dibenzyl complex is shown; for the synthesis of the analogous di-*neo*-pentyl complex, see the Supporting Information). The yields of these reactions vary with the

* Corresponding author. E-mail: pld@chem.ucla.edu.

(1) Maynadie, J.; Berthet, J. C.; Thuery, P.; Ephritikhine, M. *J. Am. Chem. Soc.* **2006**, *128*, 1082–1083.
(2) Evans, W. J.; Kozimor, S. A.; Ziller, J. W. *Science* **2005**, *309*, 1835–1838.
(3) Diaconescu, P. L.; Arnold, P. L.; Baker, T. A.; Mindiola, D. J.; Cummins, C. C. *J. Am. Chem. Soc.* **2000**, *122*, 6108–6109.
(4) Castro-Rodriguez, I.; Nakai, H.; Zakharov, L. N.; Rheingold, A. L.; Meyer, K. *Science* **2004**, *305*, 1757–1759.
(5) Summerscales, O. T.; Cloke, F. G. N.; Hitchcock, P. B.; Green, J. C.; Hazari, N. *Science* **2006**, *311*, 829–831.
(6) Hayton, T. W.; Boncella, J. M.; Scott, B. L.; Palmer, P. D.; Batista, E. R.; Hay, P. J. *Science* **2005**, *310*, 1941–1943.
(7) Marks, T. J.; Fragala, I. L., Eds. *Fundamental and Technological Aspects of Organo-f-Element Chemistry*; Kluwer: Dordrecht, The Netherlands, 1985; Vol. 155.
(8) Bruno, J. W.; Stecher, H. A.; Morss, L. R.; Sonnenberger, D. C.; Marks, T. J. *J. Am. Chem. Soc.* **1986**, *108*, 7275–7280.
(9) Marks, T. J.; Seyam, A. M.; Kolb, J. R. *J. Am. Chem. Soc.* **1973**, *95*, 5529–5539.
(10) Marks, T. J.; Seyam, A. M. *J. Am. Chem. Soc.* **1972**, *94*, 6545–6546.
(11) Manriquez, J. M.; Fagan, P. J.; Marks, T. J.; Day, C. S.; Day, V. W. *J. Am. Chem. Soc.* **1978**, *100*, 7112–7114.
(12) Fagan, P. J.; Manriquez, J. M.; Maatta, E. A.; Seyam, A. M.; Marks, T. J. *J. Am. Chem. Soc.* **1981**, *103*, 6650–6667.
(13) Brandi, G.; Brunelli, M.; Lugli, G.; Mazzel, A. *Inorg. Chim. Acta* **1973**, *7*, 319–322.
(14) Jantunen, K. C.; Haftbaradaran, F.; Katz, M. J.; Batchelor, R. J.; Schatte, G.; Leznoff, D. B. *Dalton Trans.* **2005**, 3083–3091.
(15) Jantunen, K. C.; Batchelor, R. J.; Leznoff, D. B. *Organometallics* **2004**, *23*, 2186–2193.
(16) Berthet, J.-C.; Le Marechal, J.-F.; Ephritikhine, M. *J. Organomet. Chem.* **1994**, *480*, 155–161.
(17) Arliguie, T.; Baudry, D.; Berthet, J. C.; Ephritikhine, M.; Lemarechal, J. F. *New J. Chem.* **1991**, *15*, 569–570.
(18) Gradoz, P.; Baudry, D.; Ephritikhine, M.; Lance, M.; Nierlich, M.; Vigner, J. *J. Organomet. Chem.* **1994**, *466*, 107–118.
(19) Shafir, A.; Arnold, J. *J. Am. Chem. Soc.* **2001**, *123*, 9212–9213.
(20) Seyferth, D.; Hames, B. W.; Rucker, T. G.; Cowie, M.; Dickson, R. S. *Organometallics* **1983**, *2*, 472–474.
(21) Akabori, S.; Kumagai, T.; Shirahige, T.; Sato, S.; Kawazoe, K.; Tamura, C.; Sato, M. *Organometallics* **1987**, *6*, 2105–2109.
(22) Akabori, S.; Kumagai, T.; Shirahige, T.; Sato, S.; Kawazoe, K.; Tamura, C.; Sato, M. *Organometallics* **1987**, *6*, 526–531.
(23) Sato, M.; Suzuki, K.; Asano, H.; Sekino, M.; Kawata, Y.; Habata, Y.; Akabori, S. *J. Organomet. Chem.* **1994**, *470*, 263–269.
(24) Avens, L. R.; Bott, S. G.; Clark, D. L.; Sattelberger, A. P.; Watkin, J. G.; Zwick, B. D. *Inorg. Chem.* **1994**, *33*, 2248–2256.
(25) Monreal, M. J.; Carver, C. T.; Diaconescu, P. L. *Inorg. Chem.* **2007**, *46*, 7226–7228.
(26) Diaconescu, P. L.; Cummins, C. C. *J. Am. Chem. Soc.* **2002**, *124*, 7660–7661.
(27) Odom, A. L.; Arnold, P. L.; Cummins, C. C. *J. Am. Chem. Soc.* **1998**, *120*, 5836–5837.

10.1021/om700541u CCC: $40.75
Publication on Web 03/25/2008

Scheme 1. Syntheses of fc(NSi^{t}BuMe$_2$)$_2$UBz$_2$, 1-Bz$_2$, and [fc(NSi^{t}BuMe$_2$)$_2$UBz(OEt$_2$)][BPh$_4$], [1-Bz(OEt$_2$)][BPh$_4$]

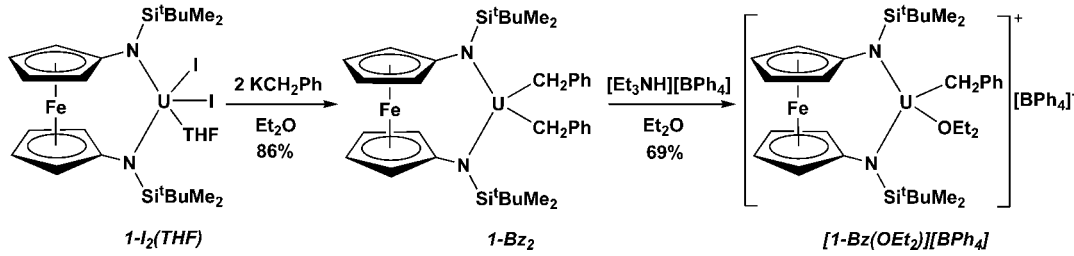

solubility of the products in nonpolar solvents, but fc(NSi^{t}BuMe$_2$)$_2$UBz$_2$, **1-Bz$_2$** (Bz = CH_2Ph) could be obtained in 86% yield after recrystallization. The X-ray crystal structure of **1-Bz$_2$** was not of very good quality and therefore discussion of the structural parameters is not attempted here. It was of reasonable quality though to indicate atom connectivity (see the Supporting Information). The only other reported actinide(IV) dialkyl complexes supported by dianionic, noncyclopentadienyl ligands are [(^{DIPP}NCOCN)U(CH_2SiMe_3)$_2$] and [(^{tBu}NON)-MR_2] (M = Th or U; R = C_3H_5 or CH_2SiMe_3; ^{DIPP}NCOCN = O(CH_2CH_2NAr)$_2$; ^{tBu}NON = O($SiMe_2N^tBu$)$_2$; Ar = 2,6-diisopropylphenyl),[14,15] and [LTh(CH_2SiMe_3)$_2$] (L = 2,6-bis(2,6-diisopropylanilidomethyl)pyridine, 4,5-bis(2,6-diisopropylanilino)-2,7-di*tert*-butyl-9,9-dimethylxantheno).[28]

With the dibenzyl uranium complex in hand, we set out to investigate the formation of a cationic complex. Alkyl cationic uranium complexes are not numerous,[29] presumably because of their high reactivity. The reaction between **1-Bz$_2$** and [Et_3NH][BPh_4] led to [fc(NSi^{t}BuMe$_2$)$_2$U(CH_2Ph)(OEt_2)][BPh_4] (**[1-Bz(OEt$_2$)][BPh$_4$]**), which was recrystallized from Et_2O/toluene. The X-ray crystal structure of **[1-Bz(OEt$_2$)][BPh$_4$]** (Figure 1) shows an η^2-coordination of the benzyl group and a pseudotetrahedral coordination around uranium (if contacts with iron and the *ipso*-carbon atoms, ca. 2.8 Å, are ignored). The U−Fe distance of 3.08 Å is similar to the Ti−Fe distance of 3.07 Å in [fc($NSiMe_3$)$_2$TiMe][$MeBPh_3$];[19] the uranium ionic radius being larger than that of titanium (1.00 Å vs 0.74 Å),[30] this distance indicates a stronger interaction of iron with uranium than with titanium. Since both metal complexes are alkyl cations, the stronger interaction with uranium is in accord with its higher Lewis acidity than that of titanium. The zirconium−iron distance in a similar alkyl cation complex, [fc($NSiMe_3$)$_2$ZrCH_2Ph]-[$PhCH_2B(C_6F_5)_3$], is 3.20 Å, more than 0.1 Å longer than the distance found in **[1-Bz(OEt$_2$)][BPh$_4$]**.[31] Examples of iron−late transition metal center interactions in complexes of 1,1′-substituted ferrocene ligands have been previously reported and also probed by X-ray crystallography.[20–23] Other metrical parameters in **[1-Bz(OEt$_2$)][BPh$_4$]** agree with reported examples; the average uranium−nitrogen distance of 2.20 Å is similar to uranium−nitrogen$_{amide}$ distances in other cationic complexes: 2.17 Å in [(η^5-C_5Me_5)$_2$U(NEt_2)(THF)$_2$][BPh_4],[32] 2.18 Å in [(η^8-C_8H_8)U(NEt_2)(THF)$_2$][BPh_4],[33] and 2.22 Å in [(η^5-C_5Me_5)$_2$U(NMe_2)(CN^tBu)$_2$][BPh_4].[34] The U−C_{benzyl} distance of 2.48 Å is slightly longer than the U−C_{Me} distance of 2.39 Å in [(η^5-C_5Me_5)$_2$UMe(THF)][$MeBPh_3$];[29] the shortening of distances involving methyl groups has been reported before.[35] The Fe−C distances average 2.07 Å, closer in value to those in ferrocenium[36] complexes rather than in ferrocene; in the latter averaged distances are closer to 2.04 Å.[37,38] The distances observed in **[1-Bz(OEt$_2$)][BPh$_4$]** likely reflect the cationic nature of the complex. One interesting feature is the fact that the uranium atom sits slightly out of the plane formed by the two nitrogens and the two carbons connected to them (dihedral angles: C10−U1−N1−C5, 17.7° and C5−U1−N2−C10, 6.5°); such a geometrical characteristic has been correlated to π-bonding with the nitrogen atoms in other chelating diamide complexes.[39,40]

To gain more insight into the nature of the iron−uranium interaction we turned to DFT calculations. Geometry optimizations were performed on model methyl compounds. The calculated iron−uranium distance is smaller for the alkyl cation model [fc($NSiH_3$)$_2$U(CH_3)(OMe_2)]$^+$ (3.04 Å) than for the dialkyl

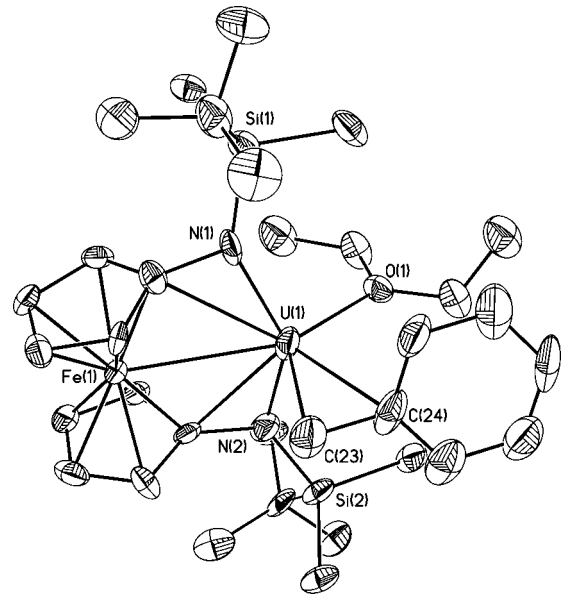

Figure 1. ORTEP representation of [fc(NSi^{t}BuMe$_2$)$_2$U(CH_2Ph)-(OEt_2)][BPh_4] (**[1-Bz(OEt$_2$)][BPh$_4$]**) with thermal ellipsoids at 35% probability. Hydrogen atoms and disordered counterparts of some atoms were omitted for clarity. The U−Fe distance is 3.08 Å. Selected uranium distances (Å): U(1)−Fe(1), 3.0714(16); U(1)−N(1), 2.169(10); U(1)−N(2), 2.236(11); U(1)−C(23), 2.482(12); U(1)−O(1), 2.4112(63). Iron−carbon distances (Å): 2.031(11); 2.052(10); 2.054(11); 2.056(12); 2.062(11); 2.0638(97); 2.069(12); 2.073(14); 2.092(10); 2.112(10). Selected angles (deg): N(1)−U(1)−N(2), 140.5(3); C(23)−U(1)−N(1), 100.7(4); C(23)−U(1)−N(2), 96.9(5); C(23)−U(1)−Fe(1), 93.0(3); N(1)−U(1)−O(1), 105.6(3); N(2)−U(1)−O(1), 90.4(3); C(23)−U(1)−O(1), 128.0(3).

(28) Cruz, C. A.; Emslie, D. J. H.; Harrington, L. E.; Britten, J. F.; Robertson, C. M. *Organometallics* **2007**, *26*, 692–701.
(29) Evans, W. J.; Kozimor, S. A.; Ziller, J. W. *Organometallics* **2005**, *24*, 3407–3412.
(30) Shannon, R. *Acta Cryst. A* **1976**, *32*, 751–767. See also http://abulafia.mt.ic.ac.uk/shannon/.
(31) Shafir, A.; Arnold, J. *Organometallics* **2003**, *22*, 567–575.
(32) Berthet, J. C.; Boisson, C.; Lance, M.; Vigner, J.; Nierlich, M.; Ephritikhine, M. *J. Chem. Soc., Dalton Trans.* **1995**, 3027–3033.
(33) Boisson, C.; Berthet, J. C.; Ephritikhine, M.; Lance, M.; Nierlich, M. *J. Organomet. Chem.* **1996**, *522*, 249–257.
(34) Boisson, C.; Berthet, J. C.; Lance, M.; Nierlich, M.; Ephritikhine, M. *J. Organomet. Chem.* **1997**, *548*, 9–16.
(35) Diaconescu, P. L.; Odom, A. L.; Agapie, T.; Cummins, C. C. *Organometallics* **2001**, *20*, 4993–4995.

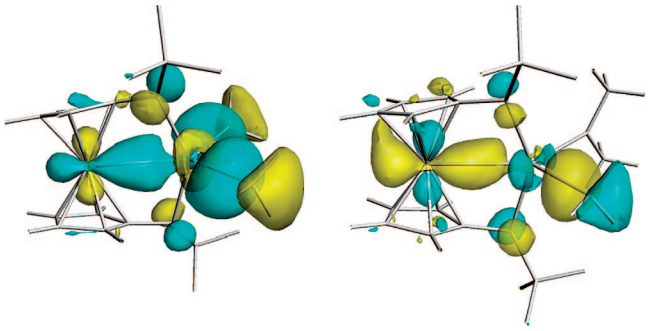

Figure 2. SOMO-6 of $fc(NSiH_3)_2U(CH_3)_2$ (left) and SOMO-5 of $[fc(NSiH_3)_2U(CH_3)(OMe_2)]^+$ (right) from geometry optimizations performed with ADF2007.01.

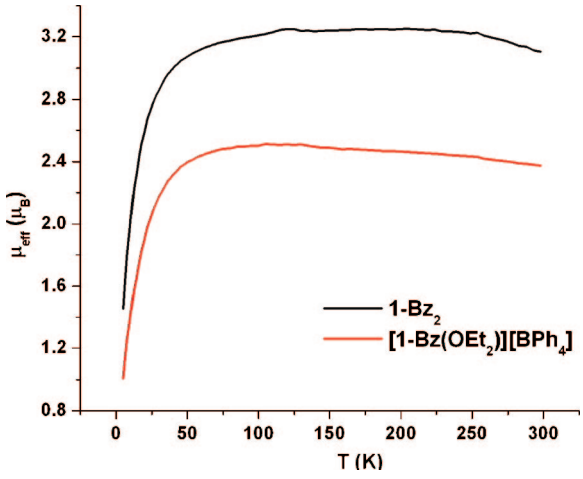

Figure 3. Plot of μ_{eff} vs T for $1\text{-}Bz_2$ and $[1\text{-}Bz(OEt_2)][BPh_4]$.

model $fc(NSiH_3)_2U(CH_3)_2$ (3.10 Å), similar to the trend observed experimentally (3.08 vs 3.18 Å). Both model complexes present one molecular orbital with an iron−uranium interaction (Figure 2). The nature[41] of these interactions is very similar to that of zirconium− or thorium−platinum interactions,[42–44] being of donor–acceptor type. In the zirconium− or thorium−platinum interactions, a molecular orbital with contributions only from the two metal centers was found; in the present case contributions from ligand atomic orbitals are also observed (Figure 2), making comparison with the reported examples not possible.

We also investigated the magnetic properties of **[1-Bz-(OEt$_2$)][BPh$_4$]**. Analyzing the magnetic moments for **[1-Bz-(OEt$_2$)][BPh$_4$]** and **1-Bz$_2$** in the temperature range 50–300 K (Figure 3), we noticed that the value corresponding to the uranium benzyl cation is considerably less than that corresponding to **1-Bz$_2$** (ca. 2.4 vs 3.2 μB). For uranium compounds, a smaller value of the room temperature magnetic moment than the one calculated for the free ion is a consequence of partly quenching the orbital-angular momentum either because of a lower symmetry or higher covalency than for the free ion ($^3H_4$ for U(IV)).[45] Since **[1-Bz(OEt$_2$)][BPh$_4$]** and **1-Bz$_2$** feature similar coordination environments, we propose that the lower magnetic moment for **[1-Bz(OEt$_2$)][BPh$_4$]** than for **1-Bz$_2$** might be consistent with the fact that the iron−uranium distance is smaller in the uranium benzyl cation than in the uranium dibenzyl complex, allowing for a better orbital overlap in the former than in the latter case.

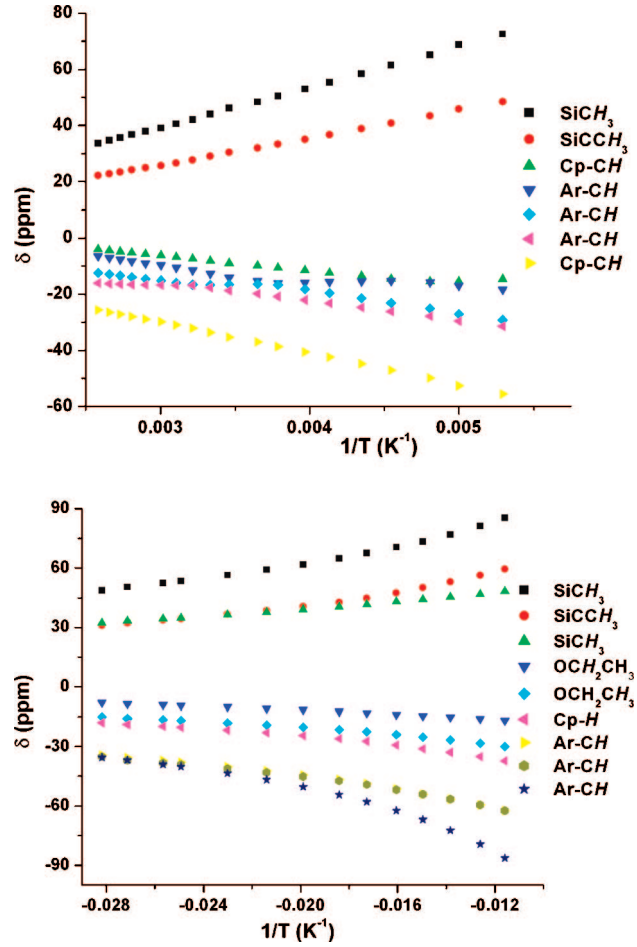

Figure 4. Chemical shift (δ) vs $1/T$ plot of the ^{1}H NMR resonances for **1-Bz$_2$** (top, from –80 to 75 °C) and **[1-Bz(OEt$_2$)][BPh$_4$]** (bottom, from –85 to 115 °C) in toluened-d_8.

To characterize further the dibenzyl and benzyl cation uranium complexes, we collected variable-temperature (VT) ^{1}H NMR spectroscopic data (Figure 4). For both complexes, **1-Bz$_2$** and **[1-Bz(OEt$_2$)][BPh$_4$]**, nonlinear dependence of the chemical shifts (δ) versus $1/T$ was observed. The nonlinearity is more pronounced for protons belonging to the cyclopentadienyl rings and the benzyl fragment. For some protons, which would be affected the most by the presence of unpaired electron density, the CH_2 benzyl group and some cyclopentadienyl protons (for the cationic complex), we could not trace the chemical shift over the entire range of temperature. Nonlinear dependence of

(36) Mammano, N. J.; Zalkin, A.; Landers, A.; Rheingold, A. L. *Inorg. Chem.* **1977**, *16*, 297–300.
(37) Churchill, M. R.; Lin, K. K. G. *Inorg. Chem.* **1973**, *12*, 2274–2279.
(38) Dunitz, J. D.; Orgel, L. E.; Rich, A. *Acta Crystallogr.* **1956**, *9*, 373–375.
(39) Boncella, J. M.; Wang, S.-Y. S.; Vanderlende, D. D.; Leigh Huff, R.; Abboud, K. A.; Vaughn, W. M. *J. Organomet. Chem.* **1997**, *530*, 59–70.
(40) Ketterer, N. A.; Ziller, J. W.; Rheingold, A. L.; Heyduk, A. F. *Organometallics* **2007**, *26*, 5330–5338.
(41) Bursten, B. E.; Novo-Gradac, K. J. *J. Am. Chem. Soc.* **1987**, *109*, 904–905.
(42) Hay, P. J.; Ryan, R. R.; Salazar, K. V.; Wrobleski, D. A.; Sattelberger, A. P. *J. Am. Chem. Soc.* **1986**, *108*, 313–315.
(43) Sternal, R. S.; Brock, C. P.; Marks, T. J. *J. Am. Chem. Soc.* **1985**, *107*, 8270–8272.
(44) Sternal, R. S.; Marks, T. J. *Organometallics* **1987**, *6*, 2621–2623.
(45) Castro-Rodriguez, I.; Olsen, K.; Gantzel, P.; Meyer, K. *J. Am. Chem. Soc.* **2003**, *125*, 4565–4571.

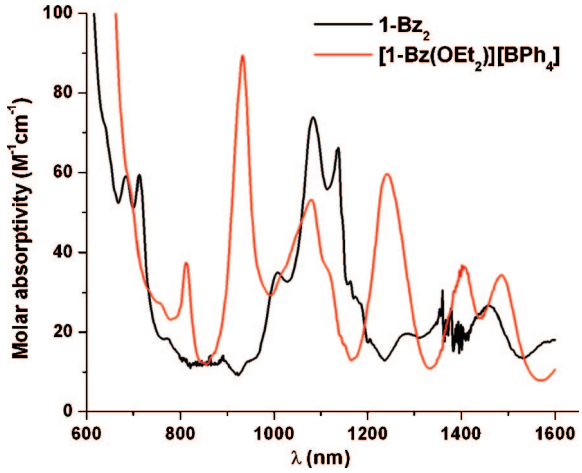

Figure 5. NIR spectra (toluene) for **1-Bz$_2$** and **[1-Bz(OEt$_2$)][BPh$_4$]**.

the chemical shift vs $1/T$[46,47] has been used as an indicator of changes in the spin density at specific protons in a complex, but the interpretation of such data is not straightforward.

The NIR spectra recorded at room temperature for both **1-Bz$_2$** and **[1-Bz(OEt$_2$)][BPh$_4$]** showed absorption bands with $\epsilon \approx 10^2$ M^{-1} cm^{-1} (Figure 5). These bands are consistent with f−f transitions;[48,49] similar spectra have been reported for $(\eta^5$-$C_5Me_5)_2UMe_2$.[50] From Figure 5 it is apparent that the NIR spectra for the two complexes are not analogous; some of the lines for the two complexes have similar shapes, but the peaks are present at rather different absorption energies. Considering that the ligands are not the same in the two complexes, it is difficult to interpret this difference in energies as a consequence of other causes.

In conclusion, a stable uranium benzyl cation complex supported by a ferrocene diamide ligand was isolated and characterized. DFT calculations and X-ray data support the existence of a weak interaction between iron and uranium.

Experimental Section

All experiments were performed under a dry nitrogen atmosphere with standard Schlenk techniques or in an MBraun inert-gas glovebox. Solvents were purified with use of a two-column solid-state purification system by the method of Grubbs[51] and transferred to the glovebox without exposure to air. NMR solvents were obtained from Cambridge Isotope Laboratories, degassed, and stored over activated molecular sieves prior to use. Uranium turnings were purchased from Argonne National Laboratories. $UI_3(THF)_4$,[24] KBz,[52] $[Et_3NH][BPh_4]$,[53] and $fc(NHSi^tBuMe_2)_2$[25] were prepared following published procedures. Other chemicals were used as received. ^{1}H NMR spectra were recorded on Bruker300 or Bruker500 spectrometers at room temperature in C_6D_6 unless otherwise specified (the UCLA NMR spectrometers are supported by NSF grant CHE-9974928). Chemical shifts are reported with respect to internal solvent, 7.16 ppm (C_6D_6). CHN analyses were performed by Desert Analytics (3860 S. Palo Verde Rd., Suite 303, Tucson, AZ 85714) and UC Berkeley Micro-Mass facility (8 Lewis Hall, College of Chemistry, University of California, Berkeley, CA 94720).

Synthesis of 1-Bz$_2$. A 20 mL scintillation vial was charged with **1-I$_2$(THF)** (0.4508 g, 0. 448 mmol) and diethyl ether (10 mL) and the suspension was cooled in a −35 °C freezer for 30 min. Benzyl potassium (KBz, 0.1223 g, 0.941 mmol) was added to the stirring suspension. The reaction mixture was stirred for 3 h, warming it to room temperature. The reaction mixture was filtered through Celite and washed with hexanes. The volatiles were removed under reduced pressure, hexanes was added to the solid, and the solution was filtered through Celite. Solvent was removed and the extraction/filtration procedure was repeated. The dried product was dissolved in hexanes and filtered through Celite one final time, concentrated, and set to crystallize at −35 °C overnight. Total yield (over three crops): 86%. ^{1}H NMR (C_6D_6, 300 MHz, 25 °C): δ, 44.79 (s, 12H, SiCH_3), 29.53 (s, 18H, SiCCH_3), −8.30 (s, 4H, Cp−CH), −12.91 (t, J = 6.42 Hz, 2H, Ar−CH), −16.79 (s, 4H, Ar−CH), −17.84 (s, 4H, Ar−CH), −34.10 (s, 4H, Cp−CH), −154.46 (s, 2H, Ar−CH_2).

Anal. Calcd for $C_{36}H_{52}FeN_2Si_2U$: C, 50.11; H, 6.14. Found: C, 50.11; H, 5.91.

Synthesis of [1-Bz(OEt$_2$)][BPh$_4$]. A concentrated toluene solution of **1-Bz$_2$** (0.1000 g, 0.116 mmol) was added to solid $[Et_3NH][BPh_4]$ (0.0488 g, 1 equiv). The reaction was stirred at room temperature for 1 h and filtered through Celite. The solvent was removed under reduced pressure and the dried product was dissolved in toluene, filtered through Celite, layered with diethyl ether, and placed in a −35 °C freezer to crystallize. Yield: 69%. ^{1}H NMR (C_6D_6, 300 MHz, 25 °C): δ, 57.23 (s, 6H, Si−CH_3), 37.12 (s, 18H, SiC(CH_3)$_3$), 36.67 (s, 6H, Si−CH_3), 24.65 (s, CH_2−Ar), 1.73 (s, 4H, OCH_2CH$_3$), −10.30 (s, 6H, OCH$_2$CH_3), −18.45 (s, 4H, Cp−H), −22.14 (s, 4H, Cp−H), −40.71 (s, 2H, Ar−H), −41.76 (s, 2H, Ar−H), −44.96 (s, 1H, Ar−H).

Anal. Calcd for $C_{57}H_{75}BFeN_2OSi_2U$: C, 59.58; H, 6.58; N, 2.44. Found: C, 60.25; H, 6.69; N, 2.17.

X-ray Crystal Structure of [1-Bz(OEt$_2$)][BPh$_4$]. X-ray quality crystals were obtained from an Et_2O/toluene solution placed in a −35 °C freezer in the glovebox. Inside the glovebox, the crystals were coated with oil (STP Oil Treatment) on a microscope slide, which was brought outside the glovebox. The X-ray data collections were carried out on a Bruker AXS single-crystal X-ray diffractometer with use of Mo Kα radiation and a SMART APEX CCD detector. The data were reduced by SAINTPLUS and an empirical absorption correction was applied, using the package SADABS. The structure was solved and refined with SHELXTL (Brucker 1998, SMART, SAINT, XPREP, and SHELXTL, Brucker AXS Inc., Madison, WI). Some atoms were disordered and therefore modeled with different occupancies over two sites. Hydrogen atoms were placed in calculated positions and refined isotropically. Crystal and refinement data for **[1-Bz(OEt$_2$)][BPh$_4$]**: formula $C_{284}H_{360}B_4N_8Si_8Fe_4U_4O_4$, space group $Pna2_1$, a = 16.1229 Å, b = 21.8507 Å, c = 18.5574 Å, $\alpha = \beta = \gamma = 90°$, V = 6537.71 Å^3, Z = 4, μ = 2.78 mm^{-1}, $F(000)$ = 2756, R_1(based on F) = 0.0689 for 9372 data ($I > 2\sigma(I)$), and wR_2(based on all data) = 0.1440.

Susceptibility Measurements. Measurements for each compound were carried out on batches obtained independently until at least two different experiments gave superimposable results. The samples used were recrystallized multiple times. Magnetic susceptibility measurements were recorded with a SQUID magnetometer at 5000 G. The samples were prepared in the glovebox (ca. 50

(46) Walter, M. D.; Berg, D. J.; Andersen, R. A. *Organometallics* **2007**, *26*, 2296–2307.
(47) Walter, M. D.; Berg, D. J.; Andersen, R. A. *Organometallics* **2006**, *25*, 3228–3237.
(48) Schelter, E. J.; Yang, P.; Scott, B. L.; Thompson, J. D.; Martin, R. L.; Hay, P. J.; Morris, D. E.; Kiplinger, J. L. *Inorg. Chem.* **2007**, *46*, 7477–7488.
(49) Clark, A. E.; Martin, R. L.; Hay, P. J.; Green, J. C.; Jantunen, K. C.; Kiplinger, J. L. *J. Phys. Chem. A* **2005**, *109*, 5481–5491.
(50) Morris, D. E.; DaRe, R. E.; Jantunen, K. C.; Castro-Rodriguez, I.; Kiplinger, J. L. *Organometallics* **2004**, *23*, 5142–5153.
(51) Pangborn, A. B.; Giardello, M. A.; Grubbs, R. H.; Rosen, R. K.; Timmers, F. J. *Organometallics* **1996**, *15*, 1518–1520.
(52) Bailey, P. J.; Coxall, R. A.; Dick, C. M.; Fabre, S.; Henderson, L. C.; Herber, C.; Liddle, S. T.; Lorono-Gonzalez, D.; Parkin, A.; Parsons, S. *Chem. Eur. J.* **2003**, *9*, 4820–4828.
(53) Dilworth, J. R.; Henderson, R. A.; Dahlstrom, P.; Nicholson, T.; Zubieta, J. A. *J. Chem. Soc., Dalton Trans.* **1987**, 529–540.

mg), loaded in a gelatin capsule that was positioned inside a plastic straw, and carried to the magnetometer in a tube under N_2. The sample was quickly inserted into the instrument and centered and data were obtained from 5 to 300 K. The contribution from the sample holders was not accounted for. Effective magnetic moments were calculated either by linear regression from plots of $1/\chi_{mol}$ versus T (K) for Curie–Weiss behavior or by using the formula $2.828(T\chi_{mol})^{1/2}$ for non-Curie–Weiss behavior.

DFT Calculations. The Amsterdam Density Functional (ADF) package (version ADF2007.01) was used to do geometry optimizations on Cartesian coordinates of the model compounds specified in the text. For the uranium and iron atoms, standard triple-ζ STA basis sets from the ADF database ZORA TZP were employed with 1s-3p (Fe) and 1s-5d (U) electrons treated as frozen cores. For all the other elements, standard double-ζ STA basis sets from the ADF database ZORA DZP or DZ were used, with the 1s electrons treated as frozen core for non-hydrogen atoms. The local density approximation (LDA) by Becke−Perdew was used together with the exchange and correlation corrections that are used by default by the ADF2007.01 program suite. Calculations for both model compounds were carried out with the spin-unrestricted, noncollinear, ZORA spin–orbit relativistic formalism.

Acknowledgment. The authors thank Dr. Saeed Khan for help with crystallography and Prof. Jeffrey Zink for allowing the use of the UV–vis−NIR spectrometer. This work was supported by the UCLA and the UC Energy Institute (EST grant).

Supporting Information Available: Experimental details for synthesis of **1-I$_2$(THF)** and **1-Np$_2$**, X-ray crystal structures of **1-I$_2$(THF)** and **1-Bz$_2$**, NIR spectra, and DFT calculation details. This material is available free of charge via the Internet at http://pubs.acs.org.

OM700541U